ELSEVIER

Journal of Photochemistry and Photobiology A: Chemistry 142 (2001) 215–220

Journal of Photochemistry and Photobiology A:Chemistry

www.elsevier.com/locate/jphotochem

Transient luminescence studies of electron injection in dye sensitised nanocrystalline TiO_2 films

Yasuhiro Tachibana [a,1], Igor V. Rubtsov [b,2], Ivan Montanari [a], Keitaro Yoshihara [b], David R. Klug [a], James R. Durrant [a,*]

[a] *Department of Chemistry, Imperial College, London SW7 2AY, UK*

[b] *School of Materials Science, Japan Advanced Institute of Science and Technology, Tatsunokuchi, Ishikawa 923-1292, Japan*

We are very pleased to dedicate this paper to Lord Porter, who provided us with such inspiration for our studies of photochemical electron transfer and energy conversion, and whose support has been invaluable to us in enabling us to conduct these studies

Abstract

We employ fluorescence upconversion spectroscopy to monitor the dynamics of electron injection in tetracarboxyphenyl zinc porphyin (ZnTCPP) sensitised nanocrystalline TiO_2 films. A good agreement is found between these measurements and previous studies of electron injection employing transient absorption spectroscopy. In both case, nonexponential kinetics are observed, with electron injection occurring on timescales ranging from <150 to ~100 ps. A simple model, based upon inhomogeneity in electron injection energetics and an exponentially increasing density of acceptor states in the metal oxide, is shown to be good agreement with the observed nonexponential injection kinetics.

1. Introduction

Photochemical approaches to solar energy conversion have attracted interest for many years. Building upon our understanding of natural photosynthesis, there have been extensive of studies of synthetic molecular redox chains designed to achieve a stable, efficient and energetic photoinduced charge separation [1]. Whilst great progress has been made towards this goal, practical applications to solar energy conversion have been limited by the difficulty in utilising the free energy stored in the charge-separated state to conduct useful work. Recently, this problem has been addressed by focusing on heterogenerous photoinduced charge separation between molecular dyes and semiconductor nanoparticles [2]. This approach has the advantage that such nanoparticles may be readily sintered together to form a porous, conducting electrode, thus allowing the photochemical charge separation reaction to be coupled to an external electrical circuit. Photoelectrochemical solar cells employing such dye sensitised nanocrystalline metal-oxide films have achieved solar to electrical energy conversion efficiencies of upto 10% [3].

The function of dye sensitised photoelectrochemical solar cells is based upon the photoinduced injection of an electron from the dye excited state into the conduction band of a wideband-gap semiconductor such as TiO_2 or ZnO [4]. The dye is generally covalently adsorbed to the metal-oxide surface, typically by the use of carboxylate groups to form ester or bidentate type bonds to surface metal sites. This electron injection process occurs on the picosecond and femtosecond timescales. In contrast, the reverse recombination process between injected electrons and oxidised dye species occurs on the micro- to milli-second timescales. This large difference between the rates of charge separation and recombination, which can be upto a factor of 10^9 [5,6], clearly favours efficient energy conversion in such solar cells. The slow recombination dynamics have been attributed to electron trapping within the metal-oxide film, and the subject of detailed numerical modelling [7].

Our own studies of the dynamics of electron injection have focused upon nanocrystalline, anatase TiO_2 sensitised by the dye ruthenium(II)*cis*-(2,2′-bipyridyl-4,4′-dicarboxylate)$_2$-$(NCS)_2$ ($Ru(dcbpy)_2(NCS)_2$). This dye/semiconductor combination is of particular technological interest in the development of dye sensitised photoelectrochemical solar cells [8]. Employing transient absorption spectroscopy, the injection kinetics were monitored by the red shift of

* Corresponding author. Fax: +44-20-7594-5801.
E-mail address: j.durrant@ic.ac.uk (J.R. Durrant).
[1] Present address: Photoreaction Control Research Centre, National Institute of Advanced Industrial Science and Technology (AIST), Central 5, 1-1-1 Higashi, Tsukuba, Ibaraki 305-8565, Japan.
[2] Present address: Department of Chemistry, University of Pennsylvania, Box 33, Philadelphia, PA 19104-6323, USA.

1010-6030/01/$ – see front matter
PII: S1010-6030(01)00516-0

a photoinduced absorption maximum in the near infrared determined from control experiments to be characteristic of formation of $Ru(dcbpy)_2(NCS)_2$ cations states [5]. The injection kinetics were observed to be nonexponential, multiexponential fits to the data required a minimum of three components with lifetimes (relative amplitudes) of <150 fs (0.30), 1 ps (0.3) and 13 ps (0.4) [5,6]. Studies employing two porphyrin dyes, zinc and free-base tetracarboxyphenyl porphyrins (ZnTCPP and H_2TCPP, respectively) yielded remarkably similar, multiexponential injection kinetics, from which it was concluded that the multiexponential behaviour most probably originated from heterogeneity of the nanocrystalline TiO_2 film [6].

Our observation of multiexponential injection kinetics contrasts with the results of several other studies. Several groups, employing a range of different dye/semiconductor samples [9–13], including the same $Ru(dcbpy)_2(NCS)_2/TiO_2$ combination employed in our own studies [11], have reported injection kinetics dominated by a single <200 fs injection phase. Recently, other groups have also reported multiphasic injection kinetics over a similar range of timescales to our own studies [14]. Determination of the parameters influencing these injection kinetics is not only of technological importance, but addresses basic scientific consideration of the appropriate models for the injection process. <200 fs injection kinetics have been modelled in terms of adiabatic electron transfer theory [15]. Alternatively, we have recently shown that non-adiabatic theory is in good agreement with the dependence of the half time of the injection kinetics upon electrical bias applied to the TiO_2 film [16].

In this paper, we extend our previous transient absorption studies of the electron injection dynamics in dye sensitised nanocrystalline TiO_2 electrodes to fluorescence upconversion studies, with the specific aim of providing further experimental support for our observation of multiphasic injection kinetics for dye sensitised nanocrystalline TiO_2 films. We then go on to discuss in detail possible origins of this multiexponential behaviour and propose a model which appears consistent with our experimental observations.

2. Materials and methods

The preparation of anatase nanocrystalline TiO_2 films (average particle diameter: 15 nm and film thickness: 8 μm) and the sensitisation of these films were conducted as described previously [6]. Following sensitisation, the films were rinsed to remove unbound dye and then covered by a drop of 50:50 propylene carbonate/ethylene carbonate under a glass cover slide. All experiments were conducted at room temperature (295 K). Steady-state absorption spectra were taken of all films after sensitisation and after the transient optical studies, all such spectra indicated that no sample degradation occurred during any of the experiments reported here.

Fluorescence upconversion measurements were carried out with the spectrometer described as previously [17]. Excitation wavelength was tuned at 614 nm with excitation power of 0.3–2.5 mW. Experiments were conducted with the sample either held stationary or traversed at sufficient speed so that each excitation pulse excited a fresh position on the sample. Results obtained under these two conditions were indistinguishable, indicating no accumulation of charge separated states nor degradation of the sample under these experimental conditions.

The time-resolved single photon counting apparatus has been described in full detail [18]. A mode-locked Coherent YAG laser synchronously pumped a DCM dye laser. The cavity dumped output had a repetition rate of 3.8 MHz and an 8 ps pulse duration. The data presented was collected with an approximately 50 ps instrument response. An excitation wavelength of 620 nm was used, and emission collected for $\lambda > 640$ nm using a 640-nm high-pass filter.

3. Results

Our fluorescence upconversion studies employed ZnTCPP sensitised nanocrystalline TiO_2 films, due to the reasonably high emission intensity observed for ZnTCPP in solution. Our previous transient absorption studies have indicated very similar injection kinetics for the ZnTCPP and $Ru(dcbpy)_2(NCS)_2$ sensitiser dyes [6]. Typical fluorescence upconversion data for ZnTCPP sensitised nanocrystalline TiO_2 films are shown in Fig. 1. Data were collected employing an excitation wavelength of 595 nm and probe wavelength of 665 nm, corresponding to absorption and emission maxima of this sensitiser dye. The fluorescence

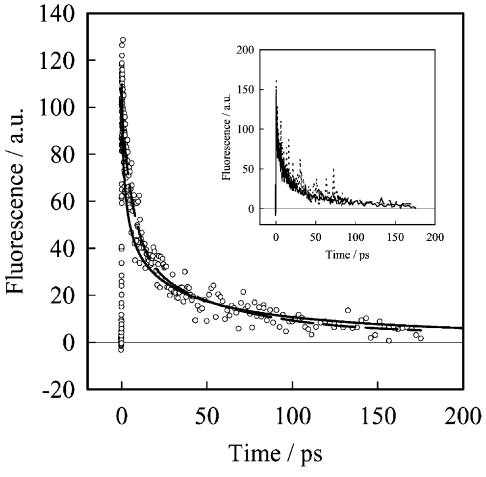

Fig. 1. Fluorescence upconversion data for ZnTCPP sensitised nanocrystalline TiO_2 films, employing excitation and probe wavelengths of 595 and 665 nm, respectively. The dashed line is a multiexponential fit to the data; the solid line is the result of a numerical simulation employing the inhomogeneous model illustrated in Fig. 4. Insert: fluorescence upconversion data as a function of laser power: 2.35 mW (—), 0.92 mW (- - -) and 0.3 mW (· · ·).

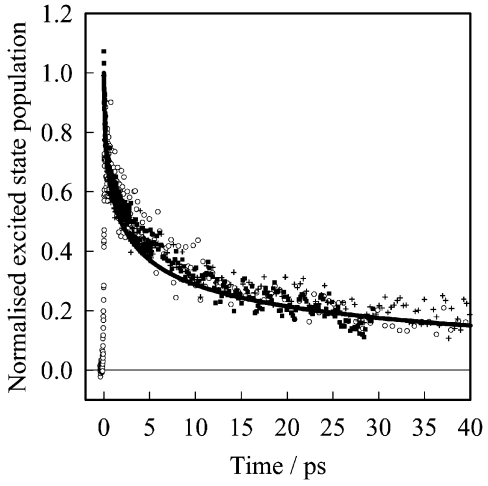

Fig. 2. Comparison of excited state decay kinetics observed in the fluorescence upconversion data shown in Fig. 1 (○), with kinetics obtained from analysis of transient absorption data for analogous ZnTCPP/TiO_2 films (●) and $Ru(dcbpy)_2(NCS)_2$/TiO_2 films (+). The solid line is result of a numerical simulation employing to the inhomogeneous model illustrated in Fig. 4. The absolute excited-state populations were determined from comparison of transient absorption spectra as function of time delay with control spectra for the dye cation and excited states.

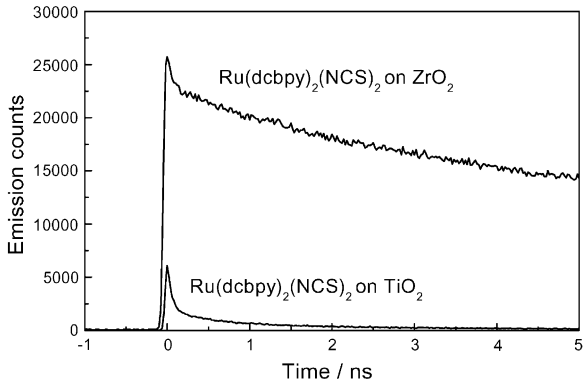

Fig. 3. Time-resolved single photon counting decays of emission from $Ru(dcbpy)_2(NCS)_2$ sensitised TiO_2 and ZrO_2 films.

decay is nonexponential; multiexponential analyses required a minimum of three components to obtain a reasonable fit to the data. These decay kinetics were found to be insensitive to laser intensity, as illustrated in the inset to this figure.

In Fig. 2, we compare these upconversion data with our previously reported transient absorption data [5,6]. Transient absorption data are shown for both the ZnTCPP and $Ru(dcbpy)_2(NCS)_2$ sensitiser dyes. Excited-state populations were determined from the transient absorption data assuming negligible decay to ground on the timescale of the experiment. It is apparent from this figure that there is an good agreement between all three data sets. We note that the limited time resolution of the upconversion data (instrument response ~300 fs) prevents the observation of the fastest (<150 fs) injection phase observed in the transient absorption data. The presence of this phase in the transient absorption data was determined from transient spectra and comparison with control data for the sensitiser dyes in solution, which indicated approximately 30% formation of dye cation states within this time period [6]. Beyond the data collection instrument response, the three datasets overlay and exhibit indistinguishable kinetics.

The upconversion and transient absorption data shown in Figs. 1–3 exhibit multiexponential excited state decay kinetics on timescales upto 200 ps. This time window was further extended by time-resolved single photon counting experiments upto the nanosecond timescale. Typical data are shown in Fig. 3, for dye sensitised TiO_2 and ZrO_2 films, in this case employing the $Ru(dcbpy)_2(NCS)_2$ dye. ZrO_2 films were employed as control samples, the relatively high conduction band edge of this material preventing electron injection, consistent with the long excited state lifetime observed for dyes adsorbed to this film [5]. It is apparent that a significant proportion (~3–5%) of the excited state decay occurs on the 100 ps to nanosecond timescales, in good agreement with the amplitude of the >200 ps component observed in the fluorescence upconversion experiment, and with previous single photon counting studies of dye sensitised metal-oxide films [19,20].

4. Discussion

The fluorescence upconversion data we report here is in good agreement with the transient absorption data we have reported previously. In particular, we find that the excited state decay exhibits multiphasic decay processes on timescales from femtoseconds to nanoseconds. Assignment of the early time decay (<100 ps) specifically to electron injection has been confirmed from transient absorption amplitude spectra. Such data determined, for example, for the case of the $Ru(dcbpy)_2(NCS)_2$ dye, that these faster phases were all associated with a red shift of a near-infrared absorption maximum characteristic of formation of dye cation species [5,6]. For longer times, the transient absorption spectra cannot be assigned so unambiguously, and dye excited state decay to ground may also contribute to the fluorescence decay kinetics.

Our observation of multiphasic injection kinetics is in contrast to the results of several other groups who have reported primarily <150 fs, injection kinetics for apparently similar dye sensitised titania films literature [11,21], although recently, other groups have also reported similar multiexponential injection kinetics [14]. The origin of this variation remains unclear. The difference may result at least in part from difference in the electronic coupling due to the sensitiser dyes employed [9]. The injection kinetics have, for example, been reported to be sensitive to the separation between the sensitiser dye and metal-oxide surface [22]. A study employing an alizarin dye, which exhibits strong

electronic coupling to the semiconductor, has reported <100 fs injection kinetics into both conduction band and sub-band gap states [13]. For the case of such fast injection kinetics, detailed analyses of the monoexponential/multiphasic nature of the kinetics are more difficult to undertake, and in any case probably not important for consideration of sensitising efficiency.

We turn now to the origin of the nonexponential, or multiphasic, injection kinetics observed in both our transient absorption and fluorescence upconversion studies of dye sensitised TiO_2 films. This multiphasic behaviour appears not to be dye specific, as similar kinetics were observed for both ruthenium bipyridyl and porphyrin dyes [6], nor dependent upon the laser power and dye coverage. On the basis of emission upconversion data, kinetic competition between electron injection and relaxation/intersystem crossing dynamics of the dye excited state has recently been suggested to result in biphasic injection kinetics for a ruthenium bipyridyl dye [12]. However, the small Stokes shift and long singlet excited state lifetime of the Zn porphyrin dye indicates that such competition is unlikely to be significant for this dye. Our observation of similar injection kinetics for both the ruthenium bipyridyl and porphyrin dyes indicates that kinetic competition with excited state dynamics is very unlikely to be the origin of the multiphasic behaviour observed in our studies. As we have discussed previously [6], the observed nonexponential behaviour most probably arises from local inhomogeneities of the TiO_2 film, consistent with for example recent single molecule emission studies of cresyl violet sensitised ITO films which indicated an inhomogeneous distribution of injection kinetics [20].

Following Fermi's golden rule, the rate of electron transfer from the dye excited state to an acceptor state in the semiconductor is given by

$$k = \frac{2\pi}{\hbar} V^2 \mathrm{FC} \tag{1}$$

where V is the electronic coupling between the states, and FC the Franck Condon factor associated with overlap of the nuclear wave functions. Determination of the overall rate of electron injection into the semiconductor requires integration over all accessible acceptor states of the semiconductor, defined by a density of states term $g(E)$ (in the absence of any applied bias, we can assume zero occupancy these states prior to electron injection).

Multiphasic injection kinetics have previously been reported for $Ru(dcbpy)_2(NCS)_2$ sensitised ZnO films by Lian and co-workers [23]. It was proposed in this paper that their observed multiphasic behaviour could derive from heterogeneity in the electronic coupling term V. Assuming a Gaussian distribution of V, a good agreement was obtained with experimental data. Employing this model to simulate our own injection data, we also obtained a reasonable fit to our data. However, this fit could only be obtained for an unreasonably large width of the Gaussian distribution of V. Specifically, a fit could only be obtained by employing a full-width at half-maximum (FWHM) of the distribution of V at least twice the magnitude of the mean value $\langle V \rangle$. Such a wide distribution implies, for example, a significant proportion of negative values of the coupling, which is clearly physically unreasonable. We conclude that, due to the broad range of timescales we observe for electron injection, a Gaussian distribution of the electronic coupling cannot alone be the origin of our observed multiphasic behaviour.

We detail here an alternative model for the origin of this multiphasic behaviour, as illustrated in Fig. 4. This model is based upon two separate considerations. Firstly, several studies have indicated that the density of conduction band/trapped electrons in nanocrystalline TiO_2 films increases exponentially with applied potential, indicative of an exponentially increasing density of states

$$g(E) \propto \exp\left(-\frac{E}{E_0}\right) \tag{2}$$

with values of the energy coefficient E_0 varying in the literature between 60 and 200 meV [7,24,25]. Secondly, electrostatic interactions at the dye/semiconductor interface are likely to result in significant local variations in the energetics of electron injection. Protonation/deprotonation of surface bound hydroxy groups induced by modulation of the electrolyte pH have been shown to result in shifts of flat band potential of nanocrystalline TiO_2 films by ~60 meV/pH unit [26]. In contact with non-aqueous electrolytes, this flat band potential has shown to be sensitive to the intercalation and/or surface binding of 'potential determining' ions including not

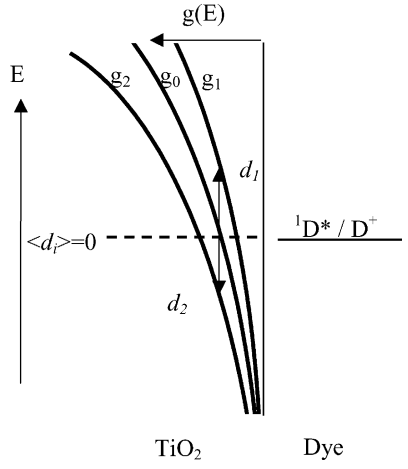

Fig. 4. Illustration of the inhomogeneous electron injection model, showing the dye excited-state energy relative to the density of TiO_2 acceptor states $g(E)$. Three different density of states are shown, the average density of states g_0, and two density of states g_1 and g_2 shifted in energy relative to the dye excited-state energy by local electrostatic interactions by energies d_1 and d_2. In the model calculations $g(E)$ is assumed to be exponential ($g(E) \propto \exp(-E/E_0)$) and the inhomogeneous energy shifts d_i selected at random following a Monte Carlo procedure from a Gaussian distribution of width Δ FWHM. We note that d_i refers to the relative energies of the dye donor and TiO_2 acceptor states, the inhomogeneous distribution of d_i may result from inhomogeneous shifts of either the dye or semiconductor states.

only protons but small-metals ions such as Li^+ [27]. Such electrostatic interactions have also been reported to modulate the redox energetics of the adsorbed sensitiser, depending upon the position of the sensitiser dye with respect to the localised charges, and extent of ionic charge screening [28,29]. Such observations are based upon macroscopic observations of film behaviour. On a microscopic level, the local charge of the metal-oxide film is expected to show significant variations, for example, due to local protonation/deprotonation of hydroxyl groups. Such local variations in charge can be expected to result in significant local variations in the energy difference between the dye excited-state oxidation potential and the semiconductor density of acceptor states $g(E)$. These two considerations, a heterogeneous distribution of local injection energetics, and an exponentially increasing $g(E)$ are illustrated in Fig. 4.

Numerical simulations were conducted based upon the model illustrated in Fig. 4, assuming a Gaussian distribution for local shifts d_i in the energies of the semiconductor acceptor states relative to the dye excited state. The experimentally observed excited state decay kinetics $N_e(t)$ were determined from:

$$N_e(t) = \frac{1}{N}\sum_{i=1}^{N} \exp(-k(d_i)t) \quad (3)$$

where d_i represents the local shift of the injection energetics, selected at random from a Gaussian probability distribution with mean 0 and width Δ. Simulations were conducted for N different values of d_i (typically $N = 1000$). $k(d_i)$ was determined from [3]:

$$k(d_i) = k(0)\frac{V^2(d_i)}{V^2(0)} = k(0)\exp\left(\frac{2d_i}{E_0}\right) \quad (4)$$

The results of these simulations depended on two fitting parameters $k(0)$ and the ratio Δ/E_0. A good agreement was found with experiment for values of $k(0) = 0.5 \times 10^{12}\,s^{-1}$ and $(\Delta/E_0) = 1.5$, as illustrated in Figs. 1 and 2. Employing literature values for E_0, this suggests values for Δ of 90–300 meV FWHM (38–125 meV standard deviation). This range of value for Δ seems reasonable, given that variations in the concentration of potential determining ions can result in shifts of the macroscopic flat band potential of the such films by over 1 eV. We conclude that this model as illustrated in Fig. 4 is consistent with the highly multiphasic injection kinetics we observe experimentally.

Our model is based upon the assumption of a density of acceptor states increasing exponentially with energy (Eq. (2)). Experimental evidence for this assumption is rather indirect, based largely upon observations of the density of trapped/conduction band electrons in nanocrystalline TiO_2 as a function of applied electrical bias. The physical origin of this exponential behaviour is moreover unclear. However we note that we have shown elsewhere, that numerical models based upon an exponentially increasing density of trap states are also in good agreement with our experimental observations of charge recombination dynamics for comparable dye sensitised metal-oxide films [7].

The analysis we present here is based upon non-adiabatic electron transfer theory. This theory is most appropriate given the timescales from electron injection reported here. We have shown elsewhere that such non-adiabatic theory is in good agreement with the dependence of the electron injection kinetics on electrical bias, interpreted as modulating the occupancy of the TiO_2 acceptor states [16].

Consideration of the local inhomogeneities in the semiconductor/dye/electrolyte interface may be important for future optimisation of device function. Optimisation of the voltage output of dye sensitised solar cells, and the use of near infrared absorbing sensitiser dyes will require careful minimisation of the free energy differences driving each stage of device function. As such, the presence of inhomogeneous broadening of these energetics may result in a significant limitation on device efficiency. For example, it is possible that the low amplitude nanosecond decay phases observed in our single photon counting data may originate from dyes adsorbed to film surfaces where the local energetics do not favour electron injection. We conclude by noting that the energetic inhomogeneity we consider here is concerned with the relative energies of the dye donor and metal oxide acceptor states. Determination of physical origin of this inhomogeneity and its minimisation are likely to assist in future optimisation of dye sensitised solar cells for photoelectrochemical solar energy conversion.

[3] For determination of $k(d_i)$ we note that in general the Franck Condom term FC and the effect of integrating over all available acceptor states may also be dependent upon d_i. However, for the specific case of an exponential density of acceptor states, FC and the effect of this integration are independent of d_i and therefore may be included in a constant $k(0)$. In this case, we need consider only the dependence of the integrated electronic coupling upon d_i, which will be proportional to the density of states at $E = d_i$,: $V(d_i) \propto g(d_i)$, as employed in Eq. (4).

Acknowledgements

We are very grateful to Dr. Pascal Comte, EPFL for preparation of nanocrystalline TiO_2 films, to Dr. Saif Haque for helpful discussions and Dr. Chris Barnett for excellent technical support. J.R. Durrant and D.R. Klug are grateful to the EPSRC for financial support.

References

[1] G. Steinberg-Yfrach, J.L. Rigaud, E.N. Durantini, A.L. Moore, D. Gust, T.A. Moore, Nature 392 (1998) 479–482.
[2] B. O'Regan, M. Grätzel, Nature 353 (1991) 737–739.
[3] M.K. Nazeeruddin, P. Pechy, T. Renouard, S.M. Zakeeruddin, R. Humphry-Baker, P. Comte, P. Liska, L. Cevey, E. Costa, V. Shklover, L. Spiccia, G.B. Deacon, C.A. Bignozzi, M. Grätzel, J. Am. Chem. Soc. 123 (2001) 1613–1624.

[4] A. Hagfeldt, M. Grätzel, Acc. Chem. Res. 33 (2000) 269–277.
[5] Y. Tachibana, J.E. Moser, M. Grätzel, D.R. Klug, J.R. Durrant, J. Phys. Chem. 100 (1996) 20056–20062.
[6] Y. Tachibana, S.A Haque, I.P. Mercer, J.R. Durrant, D.R. Klug, J. Phys. Chem. B 104 (2000) 538–547.
[7] J. Nelson, S.A. Haque, D.R. Klug, J.R. Durrant, Phys. Rev. B 63 (20) (2001) 5321–5329.
[8] M.K. Nazeeruddin, A. Kay, I. Rodicio, R. Humphry-Baker, E. Muller, P. Liska, N. Vlachopoulos, M. Grätzel, J. Am. Chem. Soc. 115 (1993) 6382–6390.
[9] J.M. Rehm, G.L. Mclendon, Y. Nagasawa, K. Yoshihara, J. Moser, M. Grätzel, J. Phys. Chem. 100 (1996) 9577–9578.
[10] B. Burfeindt, T. Hannappel, W. Storck, F. Willig, J. Phys. Chem. 100 (1996) 16463–16465.
[11] J.B. Asbury, R.J. Ellingson, H.N. Ghosh, S. Ferrere, A.J. Nozik, T. Lian, J. Phys. Chem. B 103 (1999) 3110–3119.
[12] S. Iwai, K. Hara, S. Murata, R. Katoh, H. Sugihara, H. Arakawa, J. Chem. Phys. 113 (2000) 3366–3373.
[13] R. Huber, S. Spörlein, J.E. Moser, M. Grätzel, J. Wachtveitl, J. Phys. Chem. B 104 (2000) 8995–9003.
[14] G. Benkö, M. Hilgendorff, A.P. Yartsev, V. Sundström, J. Phys. Chem. B (2001) 967–974.
[15] S. Ramakrishan, F. Willig, J. Phys. Chem. B 104 (2000) 68–77.
[16] Y. Tachibana, S.A. Haque, I.P. Mercer, J.E. Msoer, D.R. Klug, J.R. Durrant, J. Phys. Chem. B 2001, in press.
[17] I.V. Rubtsov, H. Shirota, K. Yoshihara, J. Phys. Chem. A 103 (1999) 1801–1808.
[18] P.J. Booth, B. Crystall, L.B. Giorgi, J. Barber, D.R. Klug, G. Porter, Biochim. Biophys. Acta 1016 (1990) 141–152.
[19] K. Hashimoto, M. Hiramoto, A.B.P. Lever, T. Sakata, J. Phys. Chem. 92 (1988) 1016–1018.
[20] H.P. Lu, X.S. Xie, Z. Phys. Chem. 212 (1999) 59–66.
[21] T. Hannappel, B. Burfeindt, W. Storck, F. Willig, J. Phys. Chem. B 101 (1997) 6799–6802.
[22] J. Asbury, B. Hao, E. Wang, W. Lian, J. Phys. Chem. B 104 (2000) 11957–11964.
[23] J. Asbury, B. Wang, W. Lian, J. Phys. Chem. B 103 (1999) 6643–6647.
[24] N.W. Duffy, L.M. Peter, R.M.G. Rajapakse, K.G.U. Wijayantha, Electrochem. Commun. 2 (2000) 658–662.
[25] A. Kay, M. Grätzel, J. Phys. Chem. 97 (1993) 6272–6277.
[26] G. Rothenberger, D. Fitzmaurice, M. Grätzel, J. Phys. Chem. 96 (1992) 5983–5986.
[27] G. Redmond, D. Fitzmaurice, J. Phys. Chem. 97 (1993) 1426–1430.
[28] A. Zaban, S. Ferrere, B.A. Gregg, J. Phys. Chem. B 102 (1998) 452–460.
[29] S.G. Yan, J.T. Hupp, J. Phys. Chem. B 101 (1997) 1493–1495.